

RESEARCH ARTICLE

10.1029/2017JA025003

This article is a companion to Simms et al. (2018) <https://doi.org/10.1029/2017JA025002>.

Key Points:

- Regression analyses of relativistic electron flux (0.7–7.8 MeV) show both linear and nonlinear response to wave activity
- High chorus intensity and midrange ULF Pc5 power result in more electron acceleration than would be predicted by an additive model
- The negative effect of EMIC waves is greater if combined with either chorus or ULF Pc5 waves

Correspondence to:

L. E. Simms, simmsl@augsborg.edu

Citation:

Simms, L. E., Engebretson, M. J., Clilverd, M. A., Rodger, C. J., & Reeves, G. D. (2018). Nonlinear and synergistic effects of ULF Pc5, VLF chorus, and EMIC waves on relativistic electron flux at geosynchronous orbit. *Journal of Geophysical Research: Space Physics*, 123, 4755–4766. <https://doi.org/10.1029/2017JA025003>

Received 12 NOV 2017

Accepted 6 APR 2018

Accepted article online 18 APR 2018

Published online 16 JUN 2018

Nonlinear and Synergistic Effects of ULF Pc5, VLF Chorus, and EMIC Waves on Relativistic Electron Flux at Geosynchronous Orbit

Laura E. Simms¹ , Mark J. Engebretson¹ , Mark A. Clilverd² , Craig J. Rodger³ , and Geoffrey D. Reeves⁴ 

¹Department of Physics, Augsburg University, Minneapolis, MN, USA, ²British Antarctic Survey (NERC), Cambridge, UK, ³Department of Physics, University of Otago, Dunedin, New Zealand, ⁴Los Alamos National Laboratory, Los Alamos, NM, USA

Abstract Using data covering the years 2005–2009, we study the linear and nonlinear responses of \log_{10} relativistic electron flux measured at geosynchronous orbit to ultralow frequency (ULF) Pc5, very low frequency (VLF) lower band chorus, and electromagnetic ion cyclotron (EMIC) waves. We use regression models incorporating a quadratic term and a synergistic interaction term. Relativistic electron fluxes respond to ULF Pc5 and VLF chorus waves both linearly and nonlinearly. ULF Pc5 waves contribute both to electron enhancement (at midrange wave activity) and loss (at high levels of wave activity). Nonlinear effects of VLF chorus are positive (i.e., cause acceleration), adding to the positive linear effects. Synergistic interaction effects between high levels of VLF chorus and midrange values of ULF Pc5 waves result in more electron acceleration than would be predicted by a simpler additive model. Similarly, the negative effect of EMIC waves (losses) is more influential than would be predicted by a linear model when combined with either VLF chorus or ULF Pc5 waves. During disturbed conditions (high Kp), geostationary electron flux responds more strongly to the same levels of ULF Pc5 and VLF chorus waves. This flux also responds more to ULF Pc5 and chorus waves during southward Bz conditions. Unstandardized regression coefficients for models incorporating nonlinear and synergistic effects of waves are presented for use in future modeling.

1. Introduction

At geosynchronous orbit, the level of relativistic electron flux is in part controlled by wave-particle interactions. Flux enhancement follows both enhanced ultralow frequency (ULF) Pc5 wave activity (2–7 mHz; Borovsky & Denton, 2014; Degtyarev et al., 2009; Lam, 2017; Mathie & Mann, 2000; Mann et al., 2004; O'Brien et al., 2003; Rostoker et al., 1998; Simms et al., 2016; Su et al., 2015) and very low frequency (VLF) lower band chorus wave activity (0.1–0.5 fce, the electron cyclotron frequency) (Horne et al., 2005; Iles et al., 2006; Meredith et al., 2002, 2003; Miyoshi et al., 2003, 2007; O'Brien et al., 2003; Spasojevic & Inan, 2005; Thorne et al., 2013; Turner et al., 2013, 2014). EMIC (electromagnetic ion cyclotron) waves contribute to electron loss through pitch angle scattering (Blum et al., 2015; Clilverd et al., 2007, 2015; Engebretson et al., 2015; Gao et al., 2015; Z. Li et al., 2014; Miyoshi et al., 2008; Rodger et al., 2008; Summers & Thorne, 2003; Turner et al., 2014; Usanova et al., 2014).

Co-occurring ULF Pc5 waves and a VLF chorus wave proxy have been observed to increase relativistic electron flux additively at lower L shells ($L \sim 4.5$), although ULF Pc5 effects on flux dominated over the VLF proxy at geosynchronous orbit (O'Brien et al., 2003). However, previously, we have found that VLF chorus L4 satellite observations from DEMETER (Detection of Electro-Magnetic Emissions Transmitted from Earthquake Regions) correlate well with enhanced flux at geosynchronous orbit. VLF chorus acts additively in combination with ULF Pc5 effects to produce flux enhancements (Simms et al., 2018). There has also been speculation that any loss processes associated with VLF and EMIC waves combine in their effects (Mourenas et al., 2016; Summers & Ma, 2000). Observational evidence supports this theory of additive action by VLF and EMIC waves in their ability to scatter ultrarelativistic electrons (Zhang et al., 2017).

However, the combined effect of several wave types on flux may not be simply a matter of adding their influences together. They could act synergistically, with each factor having more or less influence at varying levels of the other. This can be tested with an interaction term in multiple regression. By multiplying the factors together and entering this new variable into the analysis, the hypothesis that these factors do more than act additively can be tested.

In addition to these interactions (represented by a multiplicative factor in regression), wave effects may not be linear over their whole range. Nonlinear effects can be explored with the addition of a squared term, thereby creating a quadratic model.

Using regression techniques, we produce prediction models using wave parameters from observed data inputs, incorporating both interaction terms and quadratic terms. In this study, we use autoregressive (AR) models, to account for the high persistence of relativistic electron flux from day to day. We use data only from the day previous to the flux measurement (“lag 1”), where wave effects are strongest, and analyze only two wave types in each model so as to be able to present them graphically. In our previous analyses (Simms et al., 2018), predictor variables averaged over the day previous to that on which flux was measured (“lag 1”) correlated better with relativistic electron geostationary flux; we therefore use lag 1 predictor data for our models here. As in our previous paper, we also add an AR term: the flux on lag 1. For example, the model incorporating ULF Pc5 and VLF chorus would be represented as

$$\text{Log Flux}_t = b_0 + b_{\text{AR}} \times \text{Log Flux}_{t-1} + b_1 \times \text{ULF}_{t-1} + b_2 \times \text{ULF}_{t-1}^2 + b_3 \times \text{Chorus}_{t-1} + b_4 \times \text{Chorus}_{t-1}^2 + b_5 \times \text{ULF}_{t-1} \times \text{Chorus}_{t-1} \quad (1)$$

where b_0 is the intercept of the predicted regression line, b_{AR} the dependence of flux on its own value the day before (the autoregressive term), b_1 and b_2 the slopes of the relationship between the linear and quadratic (nonlinear component) ULF Pc5 terms with flux, b_3 and b_4 the parameters describing the dependence on the linear and quadratic values of chorus, and b_5 the coefficient describing the synergistic interaction effect of combined waves. This equation can be calculated by the ordinary least squares method (Neter et al., 1985).

We analyze all available data with this model then break the data into quiet times and disturbed times for separate analyses. We also break the data into southward and northward Bz, based on the Bz daily average.

2. Data and Methods

Over the years 2005–2009, we used daily averaged \log_{10} electron fluxes ($\log(\text{electrons}/(\text{cm}^2/\text{s}/\text{sr}/\text{keV}))$) for relativistic electrons in four energy channels: 0.7–1.8, 1.8–3.5, 3.5–6.0, and 6.0–7.8 MeV. Flux data come from the Los Alamos National Laboratory (LANL) Energetic Spectrometer for Particles (ESP) instruments located at geosynchronous orbit. ULF Pc5 was obtained from a ground-based ULF index covering local times 0500–1500 in the Pc5 range (2–7 mHz) obtained from magnetometers stationed at 60–70°N corrected geomagnetic latitude (nT^2/Hz ; Kozyreva et al., 2007). VLF lower band chorus (0.1–0.5 fce) daily averaged intensity ($\log(\mu\text{V}^2/\text{m}^2/\text{Hz})$) is from the Instrument Champ Electrique (ICE) on the DEMETER satellite (Berthelier et al., 2006). We use L 4 (4.0–4.99), the highest L shell for which there is good data coverage, averaged over the dayside passes of the satellite (LT 10:30). We use prenoon (dayside) chorus because it is found over a broader range of latitudes than premidnight (nightside) chorus (L. Y. Li et al., 2009; Thorne, 2010; Tsurutani & Smith, 1977).

Daily averages of interplanetary magnetic field (IMF) Bz and the Kp index are from the Omniweb database. Quiet times are defined as the lowest 75% of Kp measurements ($Kp < 2.3$, corresponding to the canonical Kp of <2+, 75% of the data points or 1146 days). Disturbed time is the highest 25% of Kp ($Kp > 2.3$ (>2+), 25% of the data points or 387 days). The southward Bz category contains those days on which average Bz < -0.3 (lower third, 511 days), while northward contains days where average Bz > 0.5 (upper third, 511 days).

EMIC wave power data are from the Halley, Antarctica, British Antarctic Survey (BAS) ground station located at L 4.6. We use the number of hours per day during which there was high EMIC activity ($>10^{-3} \text{ nT}^2/\text{Hz}$) in the <1-Hz band. Broadband activity was excluded.

For each of the four relativistic electron flux channels, using two wave types at a time, we perform multiple regressions with a linear and a squared term for each predictor, along with an interaction term derived from multiplying the two predictors together. The squared term fits a quadratic model to the data for each variable, while the interaction term tests the ability of one variable to influence the action of the other. As predictor data from 1 day previous (“lag 1”) correlates better with relativistic electron geostationary flux (Simms et al., 2018), we use lag 1 predictor data in these models. We also add an AR term: lag 1 flux. This

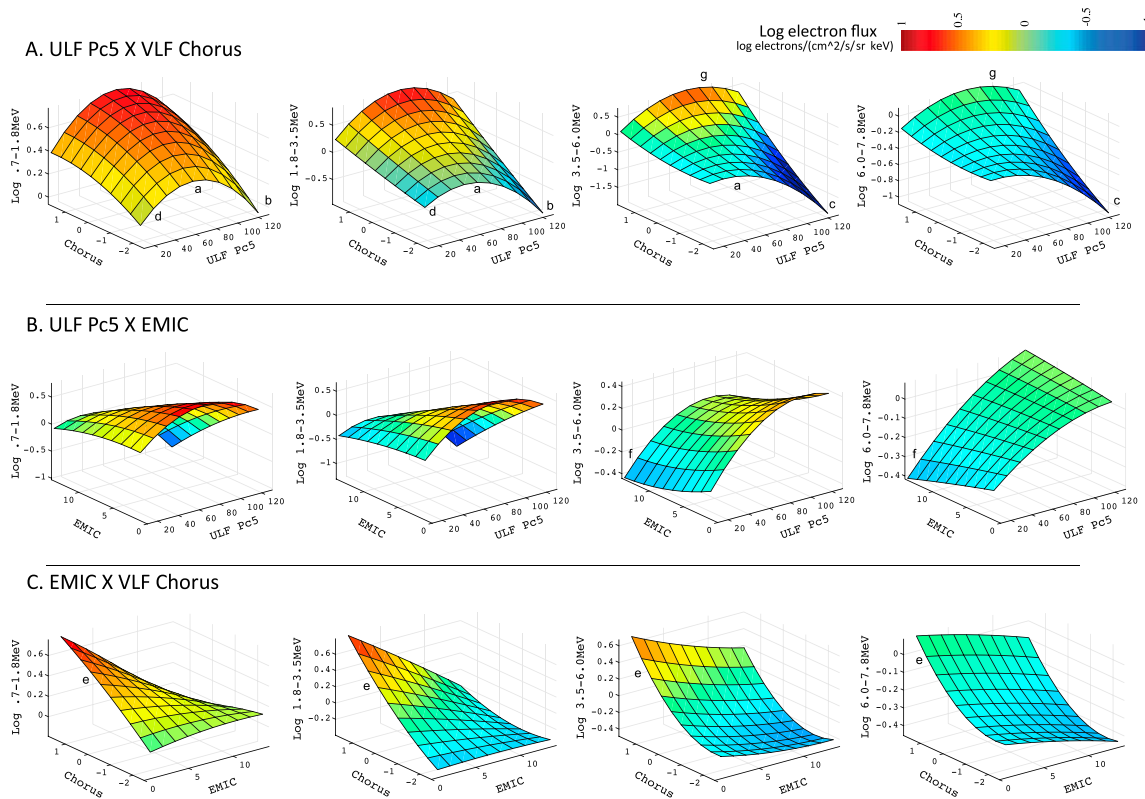


Figure 1. Linear, nonlinear, and synergistic effects between pairs of wave types. (A) ULF Pc5 and VLF chorus, (B) ULF Pc5 and EMIC, and (C) EMIC and VLF chorus. Autoregressive lag 1 models include squared and multiplicative terms that test the nonlinearity and interactive effects, respectively, for ULF Pc5 power (nT^2/Hz), lower band VLF chorus intensity ($\log(\mu\text{V}^2/\text{m}^2/\text{Hz})$), and EMIC (the number of hours per day during which there was high EMIC activity ($>10^{-3} \text{ nT}^2/\text{Hz}$) in the $<1 \text{ Hz}$ band) waves on relativistic electron flux (z axis: $\text{Log}(\text{electrons}/(\text{cm}^2/\text{s}/\text{sr}/\text{keV}))$). ULF = ultralow frequency; VLF = very low frequency; EMIC = electromagnetic ion cyclotron.

reduces the autocorrelation in the time series analysis so that the assumptions of regression analysis are not violated, as well as removing the effect of flux persistence so we can clearly see the effects of waves. We use unstandardized regression coefficients to produce the figures in order to show the influence of each variable on its own measurement scale. Graphs of the fitted regression equations (e.g., equation (1)) derived from observed data are shown in the figures. Note that the z axis (\log_{10} flux) varies between each panel. Putting them on the same scale would have obscured any patterns due to the wide variation in flux associated with each variable at each energy level. However, the color scale (showing the \log_{10} flux levels) is the same across all panels and figures.

Statistical analyses were performed in IBM SPSS Statistics, IDL, and MATLAB. Statistically significant regression coefficients (p value $< .05$ as reported in the results) mean that we have reasonable confidence that there is an actual association between the variables. The p value gives the probability that the null hypothesis is true (i.e., no association) given the distribution of the data. Thus, a low p value gives us reason to reject the null hypothesis and accept that there is an association between variables. Nonsignificant results (p value >0.05) mean we do not have enough evidence to reject this correlation between parameters (Neter et al., 1985). The setting of 0.05 as the arbitrary level for statistical significance is well established (e.g., Cowles & Davis, 1982, provide a historical perspective).

3. Results

Figure 1 shows the regression analyses for all available data. Four separate energy channels are shown on each row, with row A depicting the response of the LANL \log_{10} relativistic electron fluxes to variations in VLF chorus and ULF Pc5 wave intensity. In order to reduce congestion in the plots the units of each

Table 1
Unstandardized Regression Coefficients of the ULF Pc5 X Chorus Model

Predictors	0.7–1.8 MeV	1.8–3.5 MeV	3.5–6.0 MeV	6.0–7.8 MeV
Intercept	0.166390*	−0.239262*	−0.405719*	−0.358266*
ULF Pc5	0.014519*	0.020247*	0.018550*	0.006877*
Chorus	0.052503	0.102895	0.038928	0.017680
ULF Pc5 ²	−0.000106*	−0.000160*	−0.000176*	−0.000069*
Chorus ²	−0.019033	0.004751	0.035591*	0.016232*
ULF Pc5 X Chorus	0.000611	0.001900	0.004420*	0.001946*
Lag1 Flux (AR term)	0.774144*	0.788388*	0.896287*	0.829303*

Note. All predictors are lag 1 (measured 1 day before flux). $N = 1,534$ days. ULF = ultralow frequency; AR = autoregressive. *Effect is statistically significant ($p < 0.05$).

parameter are not added to the plot labels (but are defined in section 2 above). Row B compares the influence of EMIC and ULF Pc5 waves on the \log_{10} electron fluxes, while row C compares EMIC and VLF chorus waves.

The influence of ULF Pc5 does not follow a linear trend over its whole observed range (Figures 1A and 1B and Tables 1 and 2). The peak influence occurs at midrange powers (~ 60 nT²/Hz; letter a of Figure 1A). These trends are also visible in Figure 1B but are not labeled). Above this midrange, the influence of ULF Pc5 decreases, with the lowest influence at the highest levels of the index (b). This is described by the negative quadratic term and is strongest in the lowest three energy channels (Table 1, the coefficients of the ULF Pc5² term). However, because the positive linear effect leading to increased flux is smaller above 6.0 MeV, the major factor at this highest energy is the negative quadratic effect, resulting in a low predicted flux at the highest ULF power range (c). Below 30 nT²/Hz, ULF Pc5 influence on the lower-energy flux channels grows approximately linearly (d). The negative quadratic term describing the influence of the upper range of ULF Pc5 is more pronounced when this wave is paired with VLF chorus in the analysis (Figure 1A).

Increased VLF chorus has a positive influence on flux which is more pronounced when paired with EMIC waves (Figures 1A and 1C and Tables 1 and 3; letter e). When paired with ULF Pc5 waves, the positive VLF chorus effect on higher energies is explained mostly by the squared (nonlinear) term as shown by the significant effects of Chorus² in Table 1 compared to the nonsignificant linear effects of Chorus.

EMIC waves show an increasingly negative, mostly linear effect at higher flux energies (Figures 1B and 1C; letter f). Quadratic effects of EMIC waves are not statistically significant except at the lowest energy and when paired with ULF Pc5 (EMIC² term of Tables 2 and 3).

Waves interact synergistically in some situations. ULF Pc5 and VLF chorus mutually increase their effects (ULF Pc5 X Chorus terms of Table 1). This interaction is statistically significant at higher flux energies (3.5–7.8 MeV; terms where $p < .05$). ULF Pc5 and EMIC waves tend to depress the other's effect at the two lower channels of flux (Table 2: negative ULF Pc5 X EMIC interaction term at 0.7–1.8 and 1.8–3.5 MeV). In Figure 1B EMIC waves act to reduce low-energy electron fluxes in the presence of high ULF Pc5 wave intensities. They appear to act in synergy with ULF Pc5 waves at the highest-energy electron channels (3.5–7.8 MeV), but this effect is not

Table 2
Unstandardized Regression Coefficients of the ULF Pc5 X EMIC Model

Predictors	0.7–1.8 MeV	1.8–3.5 MeV	3.5–6.0 MeV	6.0–7.8 MeV
Intercept	−0.074965*	−0.452816*	−0.349185*	−0.320530*
ULF Pc5	0.022413*	0.028532*	0.016394*	0.005195*
EMIC	0.019205*	0.009558	−0.035587*	−0.011929*
ULF Pc5 ²	−0.000141*	−0.000164*	−0.000079*	−0.000020*
EMIC ²	−0.002066*	−0.001424	0.001171	−0.000083
ULF Pc5 X EMIC	−0.000802*	−0.000976*	−0.000111	0.000145
Lag1 Flux (AR term)	0.811735*	0.816074*	0.917664*	0.844721*

Note. All predictors are lag 1 (measured 1 day before flux). $N = 1,475$ days. ULF = ultralow frequency; EMIC = electromagnetic ion cyclotron; AR = autoregressive. *Effect is statistically significant ($p < 0.05$).

Table 3

Unstandardized Regression Coefficients of the EMIC X Chorus Model

Predictors	0.7–1.8 MeV	1.8–3.5 MeV	3.5–6.0 MeV	6.0–7.8 MeV
Intercept	0.505595*	0.243309*	0.055587*	−0.186412*
EMIC	−0.026310*	−0.038423*	−0.044165*	−0.008977
Chorus	0.208823*	0.329763*	0.280662*	0.111863*
EMIC ²	−0.000858	−0.000390	0.001046	−0.000287
Chorus ²	−0.008829	0.025636*	0.067326*	0.030831*
EMIC X Chorus	−0.020428*	−0.019829*	−0.006749	−0.000572
Lag1 Flux (AR term)	0.784324*	0.805480*	0.918211*	0.843477

Note. All predictors are lag 1 (measured 1 day before flux). $N = 1,375$ days. EMIC = electromagnetic ion cyclotron; AR = autoregressive.

*Effect is statistically significant ($p < 0.05$).

statistically significant (ULF Pc5 X EMIC terms of Table 2). In Figure 1C the EMIC waves act to quench the positive influence of increasing VLF chorus intensities, although this quenching action becomes less effective in the higher energy channels (negative EMIC X Chorus terms of Table 3).

3.1. Wave Effects During Quiet Versus Disturbed Times

To study whether wave effects during geomagnetically quiet days are different than on disturbed days, we performed the same regression analyses as above, but with data separated into low Kp (<2.3 (2+), lowest 75th percentile of daily averages) versus high Kp (>2.3 (2+), highest 25th percentile of daily averages) (Figures 2–4). The effects of wave intensity variations during quiet times are less influential. This may in part be because of a lower range of observed intensities during low Kp. In less disturbed times the ULF Pc5 index varies from 0 to 40 nT²/Hz instead of 0–125 nT²/Hz at high Kp. VLF chorus also exhibits a lower dynamic range during quiet periods to a range of −2.5 to 1 log ($\mu\text{V}^2/\text{m}^2/\text{Hz}$) versus −2 to 1.75 during high Kp. However, the range in the number of hours high power EMIC waves are observed is higher during quiet periods, with EMIC activity occurring up to 14 hr/day instead of up to 11 hr/day during high Kp. These differences in predictor ranges may affect the response of flux, most dramatically to the expanded ULF Pc5 range during disturbed times. However, it is also possible that this reflects changes in the ionosphere which influences detection of EMIC waves in the ground-based data.

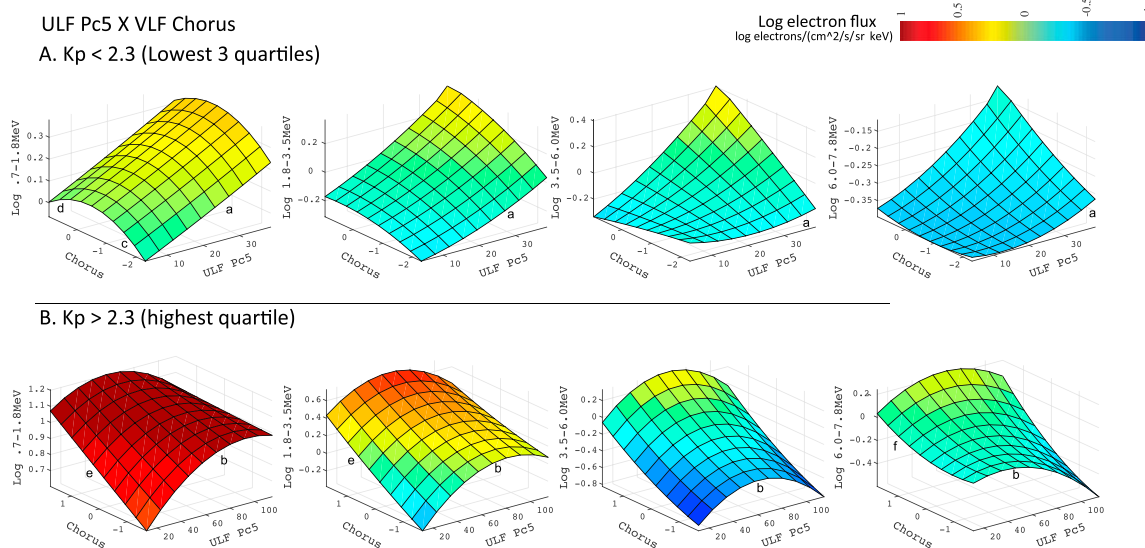


Figure 2. Linear, nonlinear, and synergistic effects of ULF Pc5 and VLF chorus waves during (A) quiet – low Kp (<2.3, lower 75th percentile) and (B) disturbed – high Kp (>2.3, upper 25th percentile). Autoregressive lag 1 models include squared and multiplicative terms that test the nonlinear and interactive effects. ULF = ultralow frequency; VLF = very low frequency.

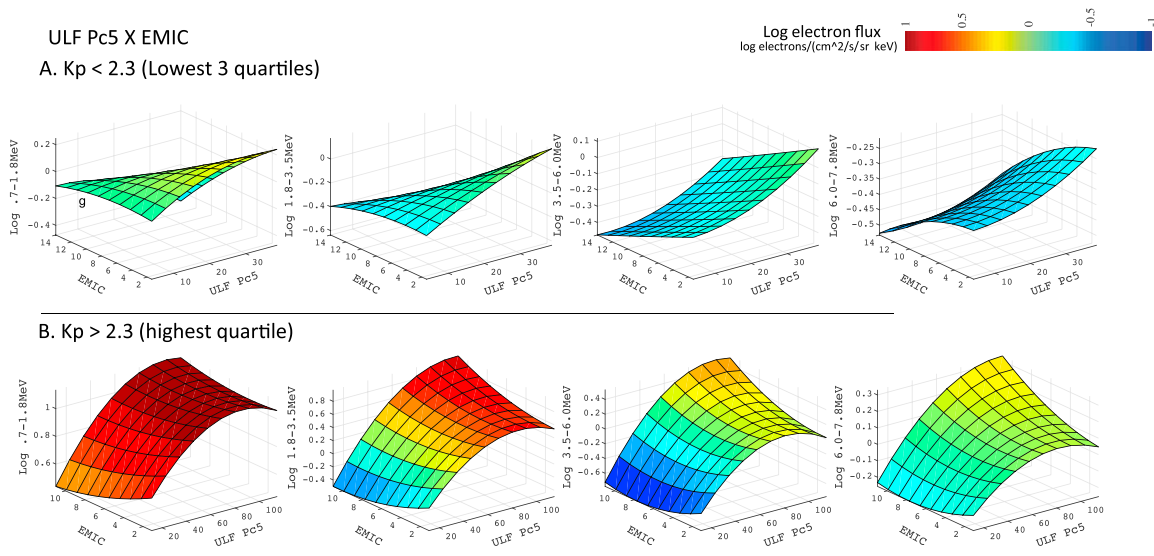


Figure 3. Linear, nonlinear, and synergistic effects of ULF Pc5 and EMIC waves during (A) quiet – low K_p (<2.3 , lower 75th percentile) and (B) disturbed – high K_p (>2.3 , upper 25th percentile). Autoregressive lag 1 models include squared and multiplicative terms that test the nonlinear and interactive effects. ULF = ultralow frequency; EMIC = electromagnetic ion cyclotron.

The response of flux at low K_p to ULF Pc5 waves is always positive (e.g., letter a, Figures 2 and 3), while at high K_p electron flux peaks during midrange ULF Pc5 values as it does in the full data set (b). However, the greater range of ULF Pc5 under high K_p conditions is not entirely responsible for the higher flux response. In the lowest energy channel (0.7–1.8 MeV) the response of flux to ULF Pc5 is higher even in the 0–40 nT²/Hz range of the ULF Pc5 index when K_p is high.

At low K_p , when VLF chorus is paired with ULF Pc5, the linear flux response is mostly positive over the energy levels (e.g., Figure 2, letter c), but a negative square term (quadratic effect) causes a leveling off of the response (a downward trend) as VLF chorus increases (e.g., letter d of Figure 2). This response is most visible at 0.7–1.8 MeV. However, at high K_p , while the response to VLF chorus is linear at the lower energies (e), the

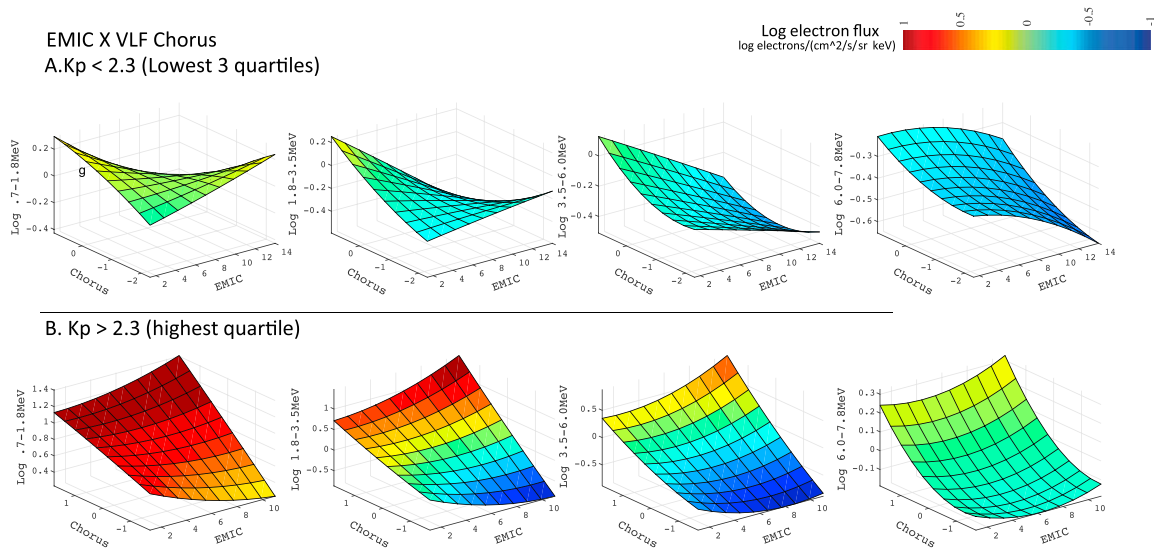


Figure 4. Linear, nonlinear, and synergistic effects of EMIC and VLF chorus waves during (A) quiet – low K_p (<2.3 , lower 75th percentile) and (B) disturbed – high K_p (>2.3 , upper 25th percentile). Autoregressive lag 1 models include squared and multiplicative terms that test the nonlinear and interactive effects. EMIC = electromagnetic ion cyclotron; VLF = very low frequency.

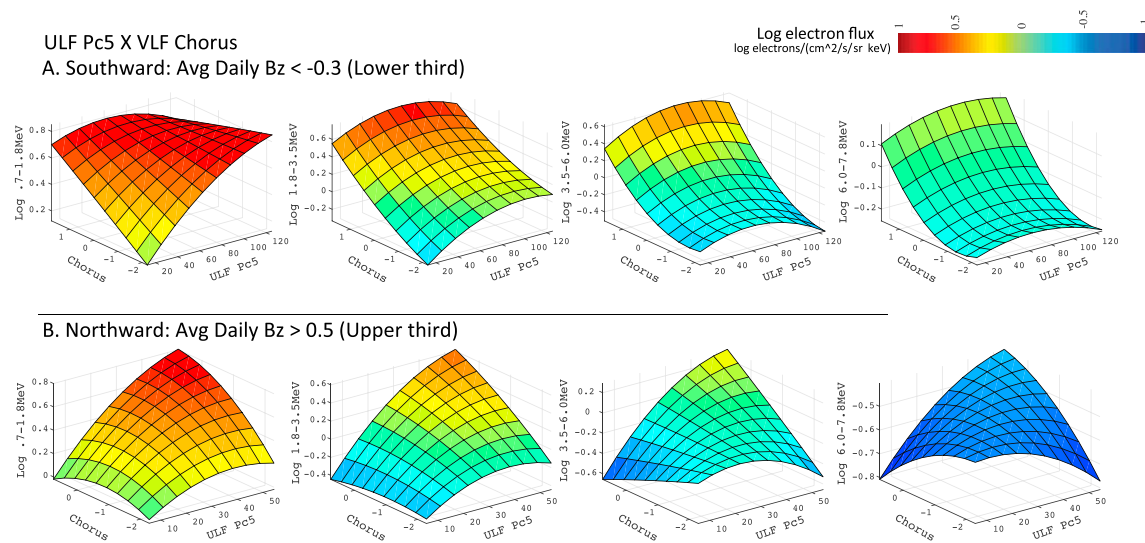


Figure 5. Linear, nonlinear, and synergistic effects of ULF Pc5 and VLF chorus waves during (A) southward Bz (daily average of Bz < −0.3) and (B) northward Bz (daily average Bz > 0.5). Autoregressive lag 1 models include squared and multiplicative terms that test the nonlinear and interactive effects. ULF = ultralow frequency; VLF = very low frequency.

positive square term (quadratic) at the higher energies becomes more influential (f), describing a more intense response to VLF chorus. This same general pattern is seen when VLF chorus is paired with EMIC waves (Figure 4).

At low Kp, the negative response of electron flux levels to EMIC waves is weak, with lower energies even showing a positive response (Figures 3 and 4, letter g).

The high Kp response for all three wave types is close to that seen in the full analysis. Most of the effect of waves in the full analysis is thus due to what occurs during disturbed conditions, but analyzing the high Kp days separately shows an even stronger flux response to wave effects. The lowest energy channel (0.7–1.8 MeV) shows a high flux at high Kp even at the lowest wave activity. This indicates that higher fluxes in this energy range are mainly due to additional processes occurring during disturbed times and not necessarily to these waves alone.

3.2. Wave Effects During Southward Vs. Northward Bz

As EMIC waves do not show dramatic nonlinear or interactive effects, we present only the ULF Pc5 X VLF Chorus model split by southward versus northward daily averaged interplanetary magnetic field Bz (Figure 5). Under conditions of more southward Bz, ULF Pc5 waves are more effective at enhancing flux in the lowest energy channels. This effect drops off at the higher energies. Even high values of ULF Pc5 result in increased flux at the lowest energy as the negative quadratic effect does not contribute appreciably. However, midrange values of ULF Pc5 wave intensity increase higher-energy flux more than the highest values of ULF Pc5 intensity. During northward Bz, the nonlinear negative effect of ULF Pc5 is stronger than during southward Bz. Increases in ULF Pc5 result in lowering of flux.

Increased VLF chorus results in increased flux at all energy levels during southward Bz, with the increases becoming more nonlinear with increased electron energy. During northward Bz, there is little effect of VLF chorus when ULF Pc5 is weak. However, as in our previous analysis, when the ULF Pc5 wave intensity is $\sim 60\text{nT}^2/\text{Hz}$ VLF chorus waves act to increase electron flux levels, particularly for the lower energy channels.

4. Discussion

In a previous paper, we studied the combined linear effects of ULF Pc5, VLF chorus, and EMIC waves on \log_{10} flux of geosynchronous orbit relativistic trapped electrons (Simms et al., 2018). In the present paper, we further this exploration by investigating the nonlinear effects of these waves, as well as possible synergistic interactions between pairs of wave types.

At all four of the energy levels studied, ULF Pc5 power is most influential when its index is at midrange values. Its influence on flux levels falls off at the highest values of the index as the negative nonlinear quadratic term in the regression model becomes more influential. At the lower flux energies in particular (0.7–3.5 MeV), the nonlinear response of flux to ULF Pc5 waves could mean that a strictly linear model would find no observed correlation with flux if a wide range of ULF Pc5 values are considered. Positive correlations with flux may only be found if ULF Pc5 waves are restricted to the lower to midrange values. This could account for conflicting results in correlations of ULF Pc5 waves with flux in earlier studies.

ULF Pc5 waves have been predicted to contribute to electron loss by outward radial diffusion during shock events (Brautigam & Albert, 2000; Degeling et al., 2008; Hudson et al., 2014; Loto'aniu et al., 2010; Shprits et al., 2006; Ukhorskiy et al., 2009; Zong et al., 2012). Although linear regression models in our previous paper only showed evidence of flux enhancement by ULF Pc5 waves and no loss (Simms et al., 2018), the nonlinear terms in our present study show that the upper range of ULF Pc5 intensities leads to reduced flux, in accord with the above studies. In our present study, ULF Pc5 induced loss is most prominent at energies >3.5 MeV. Acceleration is mainly accomplished by moderate ULF Pc5 activity (~ 60 nT²/Hz in this study), and mostly into energies between 0.7 and 3.5 MeV.

Nonlinear effects of VLF chorus are more modest, but positive. This results in more flux at the highest intensity ranges of chorus than would be expected from a strictly linear model. This has been predicted by test-particle modeling investigating the effect of large amplitude chorus (Bortnik et al., 2008; Cattell et al., 2008). VLF chorus appears more influential when ULF Pc5 is not also included in the model. This may be due to chorus (when ULF Pc5 is not present) representing the ULF Pc5 effects due to the high correlation between the two wave types. VLF chorus is most influential on the lower-energy relativistic electrons. Its reduced effect on higher energies may result from chorus also driving the compensating effect of precipitation of the most energetic electrons (Bortnik et al., 2006; Bortnik & Thorne, 2007; Hikishima et al., 2010; Lam et al., 2010; Lorentzen et al., 2001; Millan & Thorne, 2007; Orlova & Shprits, 2010).

Ozeke et al. (2017) have postulated that VLF chorus does not contribute to increased flux, as their model, using ULF wave diffusion, can adequately explain flux levels on the basis of ULF Pc5 waves alone. Jaynes et al. (2015) argued that chorus is the primary driver, at least after a depletion event. Our results show that both waves contribute to flux enhancements. Although one or the other may dominate as the primary driver in individual events, in general, we find that enhancements are driven by both waves in combination, both additively, and, at the higher energy levels, synergistically. Previous work has shown that VLF chorus and ULF Pc5 effects at geostationary orbit may add to enhance electron flux (O'Brien et al., 2003). However, the significant interaction term we see in our regression models shows that their combined action is not just additive but synergistic as well. Higher chorus levels result in more effective enhancement by midrange ULF Pc5, and vice versa. The highest flux levels are seen at high chorus intensity levels and midrange ULF Pc5 index levels. This may be the result of ULF Pc5 waves, through radial diffusion, preaccelerating electrons to subrelativistic energies. Once these electrons are at this energy level, VLF chorus waves are more effective at accelerating them to relativistic speeds.

The nonlinearity of the ULF Pc5 influence may be responsible for differing conclusions in the literature about its effectiveness relative to VLF chorus. Our results show that if ULF Pc5 occurs at low to moderate levels in a given study, a positive linear relationship between it and flux will be found. However, the inclusion of the upper range of ULF Pc5 levels in another study could lead to the conclusion that there is a negative relationship or none at all, leaving VLF chorus as the only likely seeming driver. It is also noteworthy that combining ULF Pc5 and VLF chorus in the same model results in a stronger negative effect of high intensity ULF Pc5 in the higher energy ranges. Thus, the addition of VLF chorus allows the observation of the negative ULF Pc5 quadratic effect. This demonstrates that the correlations and interactions between wave types means that studying one in isolation may not lead to valid physical interpretations of its effects. Models of these wave effects on flux on flux may benefit from using several waves as predictors and including the nonlinear quadratic effects as well as the synergistic effects between the waves.

For the most part, EMIC waves show both a less pronounced linear influence and a smaller nonlinear effect on flux. However, they do show a negative interaction with both ULF Pc5 and chorus at the lower energy levels. This negative synergism results in a larger decrease in flux when both EMIC and either ULF Pc5 or chorus waves are at high levels. Modeling work has suggested that loss processes associated with chorus could

act most effectively in conjunction with EMIC waves (Mourenas et al., 2016; Summers & Ma, 2000). There is also observational evidence that the EMIC and chorus/hiss waves act additively to decrease flux (Zhang et al., 2017). The negative interaction found in our regression models shows that the combined effect of EMIC and VLF chorus waves is not just additive. High levels of one enhance the negative action of the other. We have also found that loss due to ULF Pc5 (at high levels) is enhanced in the presence of EMIC waves in a multiplicative and not just additive manner.

The effect of all types of waves during quiet times ($K_p < 2.3$) is modest, while that during disturbed times more closely follows the patterns seen overall. Thus, most of the effects in the full analysis are due to the disturbed condition response. Some of the response difference between quiet and disturbed geomagnetic activity levels is due to different ranges of wave intensity present in these differing times. In particular, the negative nonlinear response to high levels of ULF Pc5 cannot be observed during quiet times because this wave type does not show the same high level of activity as it does during disturbed conditions. However, the initial linear slope of the low intensity ULF Pc5 effect at high K_p is steeper than that during low K_p ; thus, the effect of the same level of ULF Pc5 activity is greater during disturbed times. The same is true for VLF chorus. Chorus also shows a leveling off of effect at higher activity ($>0 \log(\mu V^2/m^2/Hz)$) during quiet times. This may indicate that precipitation due to chorus is a larger factor during quiet times.

Ground stations detect EMIC waves at a large range of L shells due to ionospheric ducting. Thus, ground data from Halley ($L = 4.6$) is useful in this study because it includes wave activity at geosynchronous orbit (Anderson et al., 1992; Kim et al., 2010, 2011). However, long-distance ionospheric ducting of EMIC waves is disrupted during disturbed times. These waves are less likely to be observed on the ground during these periods (Engebretson et al., 2008). Our study confirms this: ground-observed EMIC waves (at Halley) occur over more hours (up to 14 hr/day) during quiet times than they do during disturbed conditions (only up to 10 hr/day). Satellite observations, on the other hand, show a positive association between disturbed times and increased EMIC activity (Keika et al., 2013). This may complicate interpretations of correlations between ground-based EMIC observations and electron flux at geosynchronous orbit.

At high K_p , flux is high in the lowest energy channel (0.7–1.8 MeV) even without wave enhancements. It is likely that substorm and magnetic activity alone are responsible for much of the flux enhancements during disturbed times.

VLF chorus has a positive effect during southward B_z , but a negative effect during northward B_z . This agrees with previous findings that VLF chorus is more effective at accelerating electrons up to relativistic energies during southward B_z (Miyoshi et al., 2013). We have found the same to be true of ULF Pc5 which is more effective at enhancing flux during southward B_z conditions. Southward B_z , when reconnection is occurring, appears to be a necessary condition for the action of both VLF chorus and ULF Pc5 waves on high-energy electron flux.

5. Summary

We have undertaken a nonlinear regression analysis of the LANL geostationary trapped \log_{10} relativistic electron fluxes (0.7–7.8 MeV) in order to determine the influence of ULF Pc5, VLF, and EMIC wave intensities lagged by 1 day. We find the following:

1. The response of relativistic electron flux levels to both ULF Pc5 and VLF chorus waves can be nonlinear as well as linear. A quadratic model, therefore, may better predict flux response to these waves.
2. ULF Pc5 waves contribute both to electron enhancement (at midrange wave activity) and loss (at high levels of wave intensity). The negative (nonlinear) response at high levels of wave activity could lead to the conclusion that ULF Pc5 waves do not contribute to electron enhancement in more simplistic regression models.
3. Nonlinear effects of VLF chorus are positive. Electron flux response at high levels of chorus intensity is higher than would be predicted by a strictly linear model.
4. Synergistic interaction effects between some wave types are shown to be important. High levels of VLF chorus intensity and midrange values of ULF Pc5 wave power result in more electron acceleration than would be predicted by an additive model.
5. The negative effect of EMIC waves on flux (linked to flux decreases) is more pronounced than would be predicted by an additive linear model when combined with either chorus or ULF Pc5 waves.

6. Flux response to ULF Pc5 and VLF chorus waves varies by geomagnetic activity (Kp). During disturbed conditions, flux responds more strongly to the same level of wave intensity. In the lowest energy channel (0.7–1.8 MeV) flux at high Kp is at a high level even without wave activity enhancement.
7. Flux response to ULF Pc5 and VLF chorus waves is stronger during southward Bz conditions.
8. Unstandardized regression coefficients for models incorporating these nonlinear and synergistic effects are presented (Tables 1–3) for use in modeling.

Acknowledgments

We thank J. Bortnik, Y. Shprits, T. P. O'Brien, and an anonymous reviewer for their comments on a previous draft of this work, M. Ohnsted and N. Capman for EMIC wave identification, and R. Gamble for preparing and J.-J. Berthelier (PI) for providing DEMETER ICE data. Relativistic, seed, and source electron flux data were obtained from Los Alamos National Laboratory (LANL) geosynchronous energetic particle instruments (contact: G. D. Reeves). The ULF index is available at <http://ulf.gcras.ru/>. IMF Bz, Dst, and solar wind V, N, and P data are available from Goddard Space Flight Center Space Physics Data Facility at the OMNI Web data website (http://omniweb.gsfc.nasa.gov/html/ow_data.html). Work at Augsburg University was supported by NSF grants AGS-1264146, PLR-1341493, and AGS-1651263.

References

- Anderson, B. J., Erlandson, R. E., & Zanetti, L. J. (1992). A statistical study of Pc 1–2 magnetic pulsations in the equatorial magnetosphere. 1. Equatorial occurrence distributions. *Journal of Geophysical Research*, *97*(A3), 3075–3088. <https://doi.org/10.1029/91JA02706>
- Berthelier, J. J., Godefroy, M., Leblanc, F., Malingre, M., Menvielle, M., Lagoutte, D., et al. (2006). ICE, the electric field experiment on DEMETER. *Planetary and Space Science*, *54*(5), 456–471. <https://doi.org/10.1016/j.pss.2005.10.016>
- Blum, L. W., Halford, A., Millan, R., Bonnell, J. W., Goldstein, J., Usanova, M., et al. (2015). Observations of coincident EMIC wave activity and duskside energetic electron precipitation on 18–19 January 2013. *Geophysical Research Letters*, *42*, 5727–5735. <https://doi.org/10.1002/2015GL065245>
- Borovsky, J. E., & Denton, M. H. (2014). Exploring the cross correlations and autocorrelations of the ULF indices and incorporating the ULF indices into the systems science of the solar wind-driven magnetosphere. *Journal of Geophysical Research: Space Physics*. <https://doi.org/10.1002/2014JA019876>, *119*, 4307–4334.
- Bortnik, J., & Thorne, R. M. (2007). The dual role of ELF/VLF chorus waves in the acceleration and precipitation of radiation belt electrons. *Journal of Atmospheric and Solar-Terrestrial Physics*, *69*(3), 378–386. <https://doi.org/10.1016/j.jastp.2006.05.030>
- Bortnik, J., Thorne, R. M., & Inan, U. S. (2008). Nonlinear interaction of energetic electrons with large amplitude chorus. *Geophysical Research Letters*, *35*, L21102. <https://doi.org/10.1029/2008GL035500>
- Bortnik, J., Thorne, R. M., O'Brien, T. P., Green, J. C., Strangeway, R. J., Shprits, Y. Y., & Baker, D. N. (2006). Observation of two distinct, rapid loss mechanisms during the 20 November 2003 radiation belt dropout event. *Journal of Geophysical Research*, *111*, A12216. <https://doi.org/10.1029/2006JA011802>
- Brautigam, D. H., & Albert, J. M. (2000). Radial diffusion analysis of outer radiation belt electrons during the October 9, 1990, magnetic storm. *Journal of Geophysical Research*, *105*(A1), 291–309. <https://doi.org/10.1029/1999JA900344>
- Cattell, C., Wygant, J. R., Goetz, K., Kersten, K., Kellogg, P. J., von Rosenvinge, T., et al. (2008). Discovery of very large amplitude whistler-mode waves in Earth's radiation belts. *Geophysical Research Letters*, *35*, L01105. <https://doi.org/10.1029/2007GL032009>
- Cliiverd, M. A., Duthie, R., Hardman, R., Hendry, A. T., Rodger, C. J., Raita, T., et al. (2015). Electron precipitation from EMIC waves: A case study from 31 May 2013. *Journal of Geophysical Research: Space Physics*, *120*, 3618–3631. <https://doi.org/10.1002/2015JA021090>
- Cliiverd, M. A., Rodger, C. J., Millan, R. M., Sample, J. G., Kokorowski, M., McCarthy, M. P., et al. (2007). Energetic particle precipitation into the middle atmosphere triggered by a coronal mass ejection. *Journal of Geophysical Research*, *112*, A12206. <https://doi.org/10.1029/2007JA012395>
- Cowles, M., & Davis, C. (1982). On the origins of the .05 level of statistical significance. *American Psychologist*, *37*(5), 553–558. <https://doi.org/10.1037/0003-066X.37.5.553>
- Degeling, A. W., Ozeke, L. G., Rankin, R., Mann, I. R., & Kabin, K. (2008). Drift resonant generation of peaked relativistic electron distributions by Pc 5 ULF waves. *Journal of Geophysical Research*, *113*, A02208. <https://doi.org/10.1029/2007JA012411>
- Degtyarev, V. I., Kharchenko, I. P., Potapov, A. S., Tsegmed, B., & Chudnenko, S. E. (2009). Qualitative estimation of magnetic storm efficiency in producing relativistic electron flux in the Earth's outer radiation belt using geomagnetic pulsations data. *Advances in Space Research*, *43*(5), 829–836. <https://doi.org/10.1016/j.asr.2008.07.004>
- Engebretson, M. J., Lessard, M. R., Bortnik, J., Green, J. C., Horne, R. B., Detrick, D. L., et al. (2008). Pc1-Pc2 waves and energetic particle precipitation during and after magnetic storms: Superposed epoch analysis and case studies. *Journal of Geophysical Research*, *113*, A01211. <https://doi.org/10.1029/2007JA012362>
- Engebretson, M. J., Posch, J. L., Wygant, J. R., Kletzing, C. A., Lessard, M. R., Huang, C.-L., et al. (2015). Van Allen probes, NOAA, GOES, and ground observations of an intense EMIC wave event extending over 12 h in magnetic local time. *Journal of Geophysical Research: Space Physics*, *120*, 5465–5488. <https://doi.org/10.1002/2015JA021227>
- Gao, X., Li, W., Bortnik, J., Thorne, R. M., Lu, Q., Ma, Q., et al. (2015). The effect of different solar wind parameters upon significant relativistic electron flux dropouts in the magnetosphere. *Journal of Geophysical Research: Space Physics*, *120*, 4324–4337. <https://doi.org/10.1002/2015JA021182>
- Hikishima, M., Omura, Y., & Summers, D. (2010). Microburst precipitation of energetic electrons associated with chorus wave generation. *Geophysical Research Letters*, *37*, L07103. <https://doi.org/10.1029/2010GL042678>
- Horne, R. B., Thorne, R. M., Glauert, S. A., Albert, J. M., Meredith, N. P., & Anderson, R. R. (2005). Timescale for radiation belt electron acceleration by whistler mode chorus waves. *Journal of Geophysical Research*, *110*, A03225. <https://doi.org/10.1029/2004JA010811>
- Hudson, M. K., Baker, D. N., Goldstein, J., Kress, B. T., Paral, J., Toffoletto, F. R., & Wiltberger, M. (2014). Simulated magnetopause losses and Van Allen Probe flux dropouts. *Geophysical Research Letters*, *41*, 1113–1118. <https://doi.org/10.1002/2014GL059222>
- Iles, H. A., Meredith, N. P., Fazakerley, A. N., & Horne, R. B. (2006). Phase space density analysis of the outer radiation belt energetic electron dynamics. *Journal of Geophysical Research*, *111*, A03204. <https://doi.org/10.1029/2005JA011206>
- Jaynes, A. N., Baker, D. N., Singer, H. J., Rodriguez, J. V., Loto'aniu, T. M., Ali, A. F., et al. (2015). Source and seed populations for relativistic electrons: Their roles in radiation belt changes. *Journal of Geophysical Research: Space Physics*, *120*, 7240–7254. <https://doi.org/10.1002/2015JA021234>
- Keika, K., Takahashi, K., Ukhorskiy, A. Y., & Miyoshi, Y. (2013). Global characteristics of electromagnetic ion cyclotron waves: Occurrence rate and its storm dependence. *Journal of Geophysical Research: Space Physics*, *118*, 4135–4150. <https://doi.org/10.1002/jgra.50385>
- Kim, H., Lessard, M. R., Engebretson, M. J., & Lühr, H. (2010). Ducting characteristics of Pc 1 waves at high latitudes on the ground and in space. *Journal of Geophysical Research*, *115*, A09310. <https://doi.org/10.1029/2010JA015323>
- Kim, H., Lessard, M. R., Engebretson, M. J., & Young, M. A. (2011). Statistical study of Pc 1-2 wave propagation characteristics in the high-latitude ionospheric waveguide. *Journal of Geophysical Research*, *116*, A07227. <https://doi.org/10.1029/2010JA016355>
- Kozyreva, O., Pilipenko, V., Engebretson, M. J., Yumoto, K., Watermann, J., & Romanova, N. (2007). In search of a new ULF wave index: Comparison of Pc5 power with dynamics of geostationary relativistic electrons. *Planetary and Space Science*, *55*, 755–769.

- Lam, H.-L. (2017). On the predictive potential of Pc5 ULF waves to forecast relativistic electrons based on their relationships over two solar cycles. *Space Weather*, *15*, 163–179. <https://doi.org/10.1002/2016SW001492>
- Lam, M. M., Horne, R. B., Meredith, N. P., Glauert, S. A., Moffat-Griffin, T., & Green, J. C. (2010). Origin of energetic electron precipitation >30 keV into the atmosphere. *Journal of Geophysical Research*, *115*, A00F08. <https://doi.org/10.1029/2009JA014619>
- Li, L. Y., Cao, J. B., Zhou, G. C., & Li, X. (2009). Statistical roles of storms and substorms in changing the entire outer zone relativistic electron population. *Journal of Geophysical Research*, *114*, A12214. <https://doi.org/10.1029/2009JA01433>
- Li, Z., Millan, R. M., Hudson, M. K., Woodger, L. A., Smith, D. M., Chen, Y., et al. (2014). Investigation of EMIC wave scattering as the cause for the BARREL 17 January 2013 relativistic electron precipitation event: A quantitative comparison of simulation with observations. *Geophysical Research Letters*, *41*, 8722–8729. <https://doi.org/10.1002/2014GL062273>
- Lorentzen, K. R., Blake, J. B., Inan, U. S., & Bortnik, J. (2001). Observations of relativistic electron microbursts in association with VLF chorus. *Journal of Geophysical Research*, *106*(A4), 6017–6027. <https://doi.org/10.1029/2000JA003018>
- Loto'aniu, T. M., Singer, H. J., Waters, C. L., Angelopoulos, V., Mann, I. R., Elkington, S. R., & Bonnell, J. W. (2010). Relativistic electron loss due to ultralow frequency waves and enhanced outward radial diffusion. *Journal of Geophysical Research*, *115*, A12245. <https://doi.org/10.1029/2010JA015755>
- Mann, I. R., O'Brien, T. P., & Milling, D. K. (2004). Correlations between ULF wave power, solar wind speed, and relativistic electron flux in the magnetosphere: Solar cycle dependence. *Journal of Atmospheric and Solar-Terrestrial Physics*, *66*(2), 187–198. <https://doi.org/10.1016/j.jastp.2003.10.002>
- Mathie, R. A., & Mann, I. R. (2000). A correlation between extended intervals of ULF wave power and storm-time geosynchronous relativistic electron flux enhancements. *Geophysical Research Letters*, *27*(20), 3261–3264. <https://doi.org/10.1029/2000GL003822>
- Meredith, N. P., Cain, M., Horne, R. B., Thorne, R. M., Summers, D., & Anderson, R. R. (2003). Evidence for chorus-driven electron acceleration to relativistic energies from a survey of geomagnetically disturbed periods. *Journal of Geophysical Research*, *108*(A6), 1248. <https://doi.org/10.1029/2002JA009764>
- Meredith, N. P., Horne, R. B., Iles, R. H. A., Thorne, R. M., Heynderickx, D., & Anderson, R. R. (2002). Outer zone relativistic electron acceleration associated with substorm-enhanced whistler mode chorus. *Journal of Geophysical Research*, *107*(A7), 1144. <https://doi.org/10.1029/2001JA900146>
- Millan, R. M., & Thorne, R. M. (2007). Review of radiation belt relativistic electron losses. *Journal of Atmospheric and Solar-Terrestrial Physics*, *69*(3), 362–377. <https://doi.org/10.1016/j.jastp.2006.06.019>
- Miyoshi, Y., Kataoka, R., Kasahara, Y., Kumamoto, A., Nagai, T., & Thomsen, M. F. (2013). High-speed solar wind with southward interplanetary magnetic field causes relativistic electron flux enhancement of the outer radiation belt via enhanced condition of whistler waves. *Geophysical Research Letters*, *40*(17), 4520–4525. <https://doi.org/10.1002/grl.50916>
- Miyoshi, Y., Morioka, A., Kataoka, R., Kasahara, Y., & Mukai, T. (2007). Evolution of the outer radiation belt during the November 1993 storms driven by corotating interaction regions. *Journal of Geophysical Research*, *112*, A05210. <https://doi.org/10.1029/2006JA012148>
- Miyoshi, Y., Morioka, A., Obara, T., Misawa, H., Nagai, T., & Kasahara, Y. (2003). Rebuilding process of the outer radiation belt during the 3 November 1993 magnetic storm: NOAA and Exos-D observations. *Journal of Geophysical Research*, *108*(A1), 1004. <https://doi.org/10.1029/2001JA007542>
- Miyoshi, Y., Sakaguchi, K., Shiokawa, K., Evans, D., Albert, J., Connors, M., & Jordanova, V. (2008). Precipitation of radiation belt electrons by EMIC waves, observed from ground and space. *Geophysical Research Letters*, *35*, L23101. <https://doi.org/10.1029/2008GL035727>
- Mourenas, D., Artemyev, A. V., Ma, Q., Agapitov, O. V., & Li, W. (2016). Fast dropouts of multi-MeV electrons due to combined effects of EMIC and whistler mode waves. *Geophysical Research Letters*, *43*, 4155–4163. <https://doi.org/10.1002/2016GL068921>
- Neter, J., Wasserman, W., & Kutner, M. H. (1985). *Applied linear statistical models*, (p. 1127). Homewood, Ill: Richard D. Irwin, Inc.
- O'Brien, T. P., Lorentzen, K. R., Mann, I. R., Meredith, N. P., Blake, J. B., Fennell, J. F., et al. (2003). Energization of relativistic electrons in the presence of ULF power and MeV microbursts: Evidence for dual ULF and VLF acceleration. *Journal of Geophysical Research*, *108*(A8), 1329. <https://doi.org/10.1029/2002JA009784>
- Orlova, K. G., & Shprits, Y. Y. (2010). Dependence of pitch-angle scattering rates and loss timescales on the magnetic field model. *Geophysical Research Letters*, *37*, L05105. <https://doi.org/10.1029/2009GL041639>
- Ozeke, L. G., Mann, I. R., Murphy, K. R., Sibeck, D. G., & Baker, D. N. (2017). Ultra-relativistic radiation belt extinction and ULF wave radial diffusion: Modeling the September 2014 extended dropout event. *Geophysical Research Letters*, *44*, 2624–2633. <https://doi.org/10.1002/2017GL072811>
- Rodger, C. J., Raita, T., Clilverd, M. A., Seppälä, A., Dietrich, S., Thomson, N. R., & Ulich, T. (2008). Observations of relativistic electron precipitation from the radiation belts driven by EMIC waves. *Geophysical Research Letters*, *35*, L16106. <https://doi.org/10.1029/2008GL034804>
- Rostoker, G., Skone, S., & Baker, D. N. (1998). On the origin of relativistic electrons in the magnetosphere associated with some geomagnetic storms. *Geophysical Research Letters*, *25*(19), 3701–3704. <https://doi.org/10.1029/98GL02801>
- Shprits, Y. Y., Thorne, R. M., Friedel, R., Reeves, G. D., Fennell, J., Baker, D. N., & Kanekal, S. G. (2006). Outward radial diffusion driven by losses at magnetopause. *Journal of Geophysical Research*, *111*, A11214. <https://doi.org/10.1029/2006JA011657>
- Simms, L., Engebretson, M., Clilverd, M., Rodger, C., Lessard, M., Gjerloev, J., & Reeves, G. (2018). A distributed lag autoregressive model of geostationary relativistic electron fluxes: Comparing the influences of waves, seed and source electrons, and solar wind inputs. *Journal of Geophysical Research: Space Physics*, *123*. <https://doi.org/10.1029/2017JA025002>
- Simms, L. E., Engebretson, M. J., Pilipenko, V., Reeves, G. D., & Clilverd, M. (2016). Empirical predictive models of daily relativistic electron flux at geostationary orbit: Multiple regression analysis. *Journal of Geophysical Research: Space Physics*, *121*, 3181–3197. <https://doi.org/10.1002/2016JA022414>
- Spasojevic, M., & Inan, U. S. (2005). Ground based VLF observations near L = 2.5 during the Halloween 2003 storm. *Geophysical Research Letters*, *32*, L21103. <https://doi.org/10.1029/2005GL024377>
- Su, Z., Zhu, H., Xiao, F., Zong, Q.-G., Zhou, X.-Z., Zheng, H., et al. (2015). Ultra-low-frequency wave-driven diffusion of radiation belt relativistic electrons. *Nature Communications*, *6*(1), 10096. <https://doi.org/10.1038/ncomms10096>
- Summers, D., & Ma, C. (2000). Rapid acceleration of electrons in the magnetosphere by fast-mode MHD waves. *Journal of Geophysical Research*, *105*(A7), 15,887–15,895. <https://doi.org/10.1029/1999JA000408>
- Summers, D., & Thorne, R. M. (2003). Relativistic electron pitch-angle scattering by electromagnetic ion cyclotron waves during geomagnetic storms. *Journal of Geophysical Research*, *108*(A4), 1143. <https://doi.org/10.1029/2002JA009489>
- Thorne, R. M. (2010). Radiation belt dynamics: The importance of wave-particle interactions. *Geophysical Research Letters*, *37*, L22107. <https://doi.org/10.1029/2010GL044990>
- Thorne, R. M., Li, W., Ni, B., Ma, Q., Bortnik, J., Chen, L., et al. (2013). Rapid local acceleration of relativistic radiation-belt electrons by magnetospheric chorus. *Nature*, *504*(7480), 411–414. <https://doi.org/10.1038/nature12889>

- Tsurutani, B. T., & Smith, E. J. (1977). Two types of magnetospheric ELF chorus and their substorm dependences. *Journal of Geophysical Research*, 82(32), 5112–5128. <https://doi.org/10.1029/JA082i032p05112>
- Turner, D. L., Angelopoulos, V., Li, W., Bortnik, J., Ni, B., Ma, Q., et al. (2014). Competing source and loss mechanisms due to wave-particle interactions in Earth's outer radiation belt during the 30 September to 3 October 2012 geomagnetic storm. *Journal of Geophysical Research: Space Physics*, 119, 1960–1979. <https://doi.org/10.1002/2014JA019770>
- Turner, D. L., Angelopoulos, V., Li, W., Hartinger, M. D., Usanova, M., Mann, I. R., et al. (2013). On the storm-time evolution of relativistic electron phase space density in Earth's outer radiation belt. *Journal of Geophysical Research: Space Physics*, 118, 2196–2212. <https://doi.org/10.1002/jgra.50151>
- Ukhorskiy, A. Y., Sitnov, M. I., Takahashi, K., & Anderson, B. J. (2009). Radial transport of radiation belt electrons due to stormtime Pc5 waves. *Annales de Geophysique*, 27(5), 2173–2181. <https://doi.org/10.5194/angeo-27-2173-2009>
- Usanova, M. E., Drozdov, A., Orlova, K., Mann, I. R., Shprits, Y., Robertson, M. T., et al. (2014). Effect of EMIC waves on relativistic and ultrarelativistic electron populations: Ground-based and Van Allen Probes observations. *Geophysical Research Letters*, 41, 1375–1381. <https://doi.org/10.1002/2013GL059024>
- Zhang, X.-J., Mourenas, D., Artemyev, A. V., Angelopoulos, V., & Thorne, R. M. (2017). Contemporaneous EMIC and whistler-mode waves: Observations and consequences for MeV electron loss. *Geophysical Research Letters*, 44, 8113–8121. <https://doi.org/10.1002/2017GL073886>
- Zong, Q. G., Wang, Y. F., Zhang, H., Fu, S. Y., Zhang, H., Wang, C. R., et al. (2012). Fast acceleration of inner magnetospheric hydrogen and oxygen ions by shock induced ULF waves. *Journal of Geophysical Research*, 117, A11206. <https://doi.org/10.1029/2012JA018024>